



# Assessing the Impact of Hexavalent Chromium (Cr VI) at Varied Concentrations on *Spirulina platensis* for Growth, Metal Sorption, and Photosynthetic Responses

Adi Nath<sup>1</sup> · Abhijeet Sharma<sup>2</sup> · Shailendra Kumar Singh<sup>3</sup> · Shanthy Sundaram<sup>2</sup>

Received: 27 September 2023 / Accepted: 19 May 2024 / Published online: 19 June 2024

© The Author(s), under exclusive licence to Springer Science+Business Media, LLC, part of Springer Nature 2024

## Abstract

*Spirulina platensis*, a photosynthetic cyanobacterium, has garnered attention for its potential role in environmental remediation due to its ability to absorb and metabolize toxic heavy metals. Understanding its response toward toxicity of one of the most common contaminants, Cr(VI) is crucial for assessing its efficacy in bioremediation efforts. This study aims to investigate the physiological and biochemical responses of *Spirulina platensis* to varying concentrations of Cr(VI) from 0.5 to 5 ppm, shedding light on its potential as a bioindicator for environmental contamination and its suitability for bioremediation purposes. The impact of Cr(VI) on cell density, biosorption, pigment levels, nutrient content, fluorescence response, and photosynthetic efficiency was examined. The study revealed a gradual reduction in cell density, biomass production, and biosorption efficiency with increasing Cr(VI) concentrations. Pigment levels, carbohydrate, protein, and lipid content showed significant decreases, indicating physiological stress. Fluorescence response and photosynthetic efficiency were also adversely affected, suggesting alterations in electron transfer dynamics. A threshold for chromium toxicity was observed at 0.5 ppm, beyond which significant physiological disturbances occurred. This investigation highlights the sensitivity of *Spirulina platensis* to Cr(VI) toxicity and its potential as a bioindicator for heavy metal contamination. Metal sorption was highest in 0.5 ppm Cr(VI) with 56.56% removal. Notably, at lower concentrations, Cr(VI) acted as an intermediate electron acceptor, enhancing the electron transport chain and potentially increasing biomass under controlled conditions. The findings underscore the importance of understanding the mechanisms underlying heavy metal stress in microalgae for effective environmental remediation strategies. The research highlights the dual role of chromium(VI) in influencing *S. platensis*, depending on the concentration, and underscores the importance of understanding metal ion interactions with photosynthetic organisms for potential applications in bioremediation.

## Introduction

Chromium, a versatile transition metal, exhibits multiple oxidation states from +6 to -2, often occurring in aquatic environments as either Cr(III) or Cr(VI) depending on the pH [1]. The more toxic Cr(VI) form poses risks to proteins and DNA by generating various reactive oxygen species.

Anthropogenic activities such as mining, metal alloy and steel production, and the use of paints and dyes contribute to environmental chromium pollution, elevating the risks of soil and water contamination through waste incineration for energy [2]. This contamination escalates the risk of bio-magnification in plants and animals. Chromium(VI) interferes with photosynthesis in photosynthetic organisms by affecting the  $Q_A$ , an intermediate electron acceptor in PSII, reducing the Electron Transport Rate (ETR). The exposure could also potentially cause damage to the skin, eyes, blood, respiratory system, and immune system of animals [3, 4]. The tiny photosynthetic algal cells like cyanobacteria, exhibited a tolerance to heavy metal toxicity, making them essential for water quality management due to their diverse, oxygen-evolving capabilities and metal biosorption potential [5]. The mechanisms through which cyanobacteria mitigate heavy metal pollution in polluted water bodies are complex.

✉ Adi Nath  
adinathupadhyay@gmail.com

<sup>1</sup> Department of Botany, Nehru Gram Bharati Deemed to University, Prayagraj 221505, India

<sup>2</sup> Centre of Biotechnology, University of Allahabad, Prayagraj 211002, India

<sup>3</sup> S S Khanna Girls Degree College, Prayagraj, Uttar Pradesh 211003, India

Many researchers have shown the role of phytochelatins or metallothionein peptides in the adsorption and absorption processes [6]. Within this context, *Spirulina platensis*, a filamentous blue-green cyanobacterium belonging to the Oscillatoriaceae family, stands out as a significant primary producer in aquatic ecosystems [7].

Thus, it would be interesting to explore the novel insights into the interaction between *S. platensis* and Cr(VI), delineating the critical threshold of chromium toxicity and its multifaceted impact on the microalga's physiology, growth, and photosynthetic efficiency. By pinpointing a toxicity threshold of chromium(VI) levels, this study not only advances our understanding of metal stress on algal systems but also sheds light on the nuanced mechanisms of response and adaptation within *S. platensis*. The innovative exploration of quantum coherence and tunneling phenomena in relation to photosynthetic efficiency under metal stress introduces a novel perspective to the study of algal biology and environmental stressors [8, 9]. Furthermore, the detailed examination of chromium's effects on photosynthesis, cellular morphology, and pigment composition, alongside the potential for chromium biosorption, positions this work at the forefront of research in bioremediation technologies. This comprehensive analysis underscores the intricate balance between beneficial and detrimental impacts of chromium on *S. platensis*, offering valuable insights for environmental management and the sustainable use of algae in biotechnological applications.

## Materials and Methods

### Cyanobacteria Culture Conditions and Cr(VI) Treatment

*Spirulina platensis* (ATCC-29408), a multicellular blue-green microalga (prokaryote) was collected from the germplasm section of the Centre for Conservation and Utilisation of Blue-Green Algae (CCUBGA), Indian Agricultural Research Institute, New Delhi, India. At the Phycology Laboratory, Centre of Biotechnology, University of Allahabad, India, axenic stocks were kept on Zarrouk medium agar slants. The cyanobacteria species were grown in 250-mL flask bioreactors with Zarrouk medium (pH 7.8) and 10-mM sodium thiosulfate [10], at a constant light intensity of 60-mol photons<sup>2</sup> s<sup>-1</sup>, a temperature of 25 °C, and 50% relative humidity during the 16-h:8-h light–dark cycle. The culture media were mixed with ampicillin and streptomycin to inhibit the growth of Gram-positive and Gram-negative bacteria, respectively [11]. The use of antibiotics in cyanobacteria culture serves to maintain a sterile environment conducive to the growth and study of the target organism, minimizing the risk of experimental artifacts caused by

microbial contamination. It ensures that the observed effects are attributed solely to the cyanobacteria under investigation, thus enhancing the reliability and validity of the experimental results. To get enough biomass for the studies, cyanobacteria were sub-cultured. Triplicates of each experiment were run [12]. After the onsets of mid-log phase in the culture, the different concentrations of Cr(VI) (0.5, 1, 3, and 5 ppm) were added in the sample.

### Heavy Metal Stock Solutions

The hexavalent form of chromium, Cr(VI) was prepared by dissolving 2.75 g of K<sub>2</sub>Cr<sub>2</sub>O<sub>7</sub> (SD Fine Chemicals) in distilled water and making up the volume to 1 L. This stock solution (1000 ppm) was used in entire experiments to prepare different concentrations of Cr(VI) solution (0.5, 1.0, 3.0, and 5.0 ppm) for further analysis [10, 11].

### Determination of *S. platensis* Growth in Varying Cr(VI) Concentration

The cultures' growth was routinely monitored by measuring optical density and looking under a microscope. By measuring the optical densities, dry cell mass, and growth rates, growth performance was assessed. Cell densities were used to calculate growth rates. In brief, a 5-mL sample was taken from each culture flask on each sampling day following complete hand mixing with glass beads to obtain a homogeneous cell suspension. The optical density at 750 nm (OD<sub>750</sub>) was measured using a UV–VIS spectrophotometer (Systronics, 2202) at every alternate day, starting from day 1 and up to 20th day. The dry cell mass (DCW) of growing algal biomass was obtained by filtering 5-mL aliquots of culture through previously weighed glass microfiber (GF/C, 37 mm in diameter) filters. The weight was invariant after each loaded filter was dried at 70 °C for 24 h to remove 99% moisture from the sample. To obtain the biomass DCW, the DCW from the blank filter was subtracted from the DCW from the loaded filter.

### Chromium Biosorption by Cyanobacterial Species

To initiate the sorption studies, we prepared the required concentrations of Cr(VI) by diluting the stock solution with growth media in 500-mL Erlenmeyer flasks. The desired concentrations (0.5, 1.0, 3.0, and 5.0 ppm) were achieved by adding specific volumes of the stock solution to 200 mL of growth media in each flask. Subsequently, we introduced 10% homogenized cyanobacterial culture (w/v), prepared via homogenizer, as inoculants into the flasks. Furthermore, the flasks were placed in a controlled environment (at a constant light intensity of 60 mol photons<sup>2</sup> s<sup>-1</sup>, a temperature of 25 °C, and 50% relative humidity during the 16-h: 8-h light–dark cycle)

within a growth chamber and incubated for 14 days. Control flasks, containing growth medium inoculated with cyanobacterial culture but without Cr(VI), were subjected to the same experimental conditions as the treated flasks. After the 14-day incubation period, the biomass was separated from the medium by centrifugation at  $7000\times g$  for 20 min. The analysis of Cr(VI) uptake by the *S. platensis* biomass and the residual amount in the liquid was conducted using the diphenylcarbazide (DPC) colorimetric method after the 14 day of incubation [13]. The standard curve of the DPC method was constructed between the known concentration of Cr(VI) and absorbance at 540 nm. The graph showed a perfect fit ( $R^2=0.98$ ) up to 3-ppm Cr(VI) concentration, hence the range of this method was considered from 0 to 3 ppm. The higher concentration was estimated by the dilution method.

### Estimation of Chlorophyll-a, Carotenoid, and Phycocyanin

1.0-mL culture was taken on the late exponential phase at the duration of 14th day for the estimation of Chl-a. Centrifugation of the culture was done at  $11,200\times g$  for 10 min after that supernatant was discarded and 1-mL methanol was added in the pellet. The mixture was incubated for 30 min in deep freezer which is followed by heating in water bath for 5 min. The previous cycle was repeated 4–5 times to obtain maximum pigment. After final cycle, the mixture was centrifuged at  $2800\times g$  after which the optical density was measured at 660 nm by double-beam spectrophotometer and methanol used as a blank/reference. The obtained values multiplied with 13.42 for the yield of chl-a [14]. Total carotenoids was estimated according to [10], the carotenoid content was estimated same as per sample prepared for chl-a and optical density was measured at 460 nm by double-beam spectrophotometer and methanol used as a blank/reference. The obtained values multiplied with 12 for the yield of carotenoids. 1.0-mL culture was taken on the late exponential phase at the duration of 14th day in the Eppendorf tube for the estimation of phycocyanin. The culture was centrifuged at  $11,200\times g$  for 10 min after that supernatant was discarded and adds 1.0-mL 0.1-M potassium phosphate buffer (61.5 mL  $K_2HPO_4$  + 38.5 mL  $KH_2PO_4$ , pH 7.0) solvent in the pellet. The Eppendorf tube was wrapped with the aluminum foil and kept it in deep freezer for overnight, after that freeze and thaw cycle was repeated multiple times. Optical density was measured at 660 and 620 nm by double-beam spectrophotometer and 0.1-M potassium phosphate buffer used as a blank/reference [15]. Amount of phycocyanin was measured by the following formula:

$$\text{PhycocyaninConcentration}(\mu\text{g}/\text{mL}) = \frac{\text{OD}_{660} - (0.474) \times \text{OD}_{620}}{5.34}$$

### Measurement of Toxicity, Modulated Fluorescence, and Photosynthetic Inhibition

The initial photoluminescence saturation was measured using a Photosynthetic Efficiency Analyzer (PEA), which allows for the rapid assessment of fluorescence induction kinetics in photosynthetic organisms. The Pulse Amplitude Modulation dual-channel yield analyzer (FL-3300, Heinz Walz GmbH, Effeltrich, Germany) was used to test *Spirulina platensis*'s sensitivity in conditions supplied with various doses of Cr(VI). This technique involves exposing the sample to a saturating light pulse, followed by the measurement of fluorescence signals over time. The kinetics of fluorescence are then analyzed to extract parameters related to the efficiency and performance of the photosynthetic apparatus. The effective fluorescence yield of photosystem II (PS II) is calculated using the amplitudes of regularly spaced rectangular saturation pulses, which is a toxicity analyzer that is very sensitive to chlorophyll fluorescence. The various light types such as measuring light, saturating pulse, actinic light, far-red, variable fluorescence, and quenched fluorescence light sources were utilized for PAM analysis [16–20]. Before fluorescence analysis, an equilibrium state for the photosynthetic electron transport was induced in *S. platensis* test cultures by placing samples in completely dark conditions (by putting in the black box) for 30 min. Low-intensity modulated light was used to monitor the fluorescence in order to prevent the PSII primary electron acceptor ( $Q_A$ ) from degrading. The PAM analyzer was used to determine the impact of increasing Cr(VI) toxicity on different analytic photosynthetic parameters, including Fast Induction, Kautsky Effect,  $Q_A$ -Reoxidation, Quenching Analysis, Fluorometric Analysis, and Photosynthetic Efficiency Analyzer.

The variable/maximum fluorescence ratio ( $F_v/F_m$ ), photochemical quenching ( $Q_p$ ), and non-photochemical quenching (NPQ) were determined using the measurements of the fluorescence intensity of *S. platensis* cells activated by PAM blue light at 650 nm [21, 22].

$$\begin{aligned} \text{Effective Overall Quantum Yield}(Y) \text{ of PSII} \\ = (F_m - F_0)/F_m = F_v/F_m \end{aligned} \quad (1)$$

Relative photosynthetic inhibition is calculated using the following equations.

$$\text{Relative Photosynthetic Inhibition}(\%) = 100(Y_2 - Y_1)/Y_2(Y_1 < Y_2) \quad (2)$$

$$Q_p = (F'_M F_S) / (F'_M - F'_0) \quad (3)$$

$$\text{NPQ} = (F_M - F'_M) / F'_M \quad (4)$$

where  $F_0$  is the “Initial fluorescence at dark-adapted condition, i.e., fluorescence measured just before the application

of a saturation pulse,”  $F_m$  is the “maximum fluorescence at dark-adapted condition” (fluorescence measured during a saturation pulse),  $F_M'$  is the “maximum fluorescence at light-adapted condition,” and  $F_0'$  is the “Initial fluorescence at light-adapted condition.”

### Influence of Varying Cr(VI) Toxicity on Biochemical Composition of *S. platensis*

The test *S. platensis* species were raised in Zarrouk medium with the addition of various Cr(VI) concentrations up until the pre-stationary phase. Centrifugation was used to remove the cells from the culture broth after the proper amount of cell development (9072 g for 10 min). With deionized water, the cells were washed twice before being dried and weighed. The [23] and [24] techniques were used to calculate the estimated amounts of protein and carbohydrates in the generated biomass. A modified gravimetric technique of the [25] method was used to determine the total lipid.

### Statistical Analyses

All the experiments were conducted in the triplicates. Software called Graph Prism (version 5.0) was used for the statistical analysis and standard mean values were used to plot the graph with standard error. The significance of the results ( $P < 0.05$ ) was verified using one-way analysis of variance (ANOVA). PAST software (Version 2.17) was used to carry out the main component analysis.

## Results

### Impact of Hexavalent Chromium on *Spirulina platensis* Cell Density

Investigating the influence of varying Cr(VI) concentrations on *Spirulina platensis* revealed a gradual reduction in optical density with increased Cr(VI) toxicity, ranging from 0.5 to 5 ppm. The least decline was observed at 0.5-ppm Cr(VI), with filamentous structures, typically found below the surface, appearing atop. Growth rates showed variability with increased Cr(VI) levels, leading to an earlier commencement of the mid-log phase. At 0.5 ppm, a slight reduction in cell density suggested minimal stress ( $P < 0.05$ ) (Fig. 1a). However, the growth curve exhibited a sharp drop at higher Cr(VI) concentrations (between 1 and 5 ppm), indicating a significant level of physiological stress. Increasing the Cr(VI) concentration changed the appearance of these *Spirulina platensis* cells, a photosynthetic cyanobacterium, as seen in Supplementary Fig. 2. However, at concentrations between 1 and 5 ppm, a sharp fall in growth curves indicated considerable stress. The appearance and biomass production

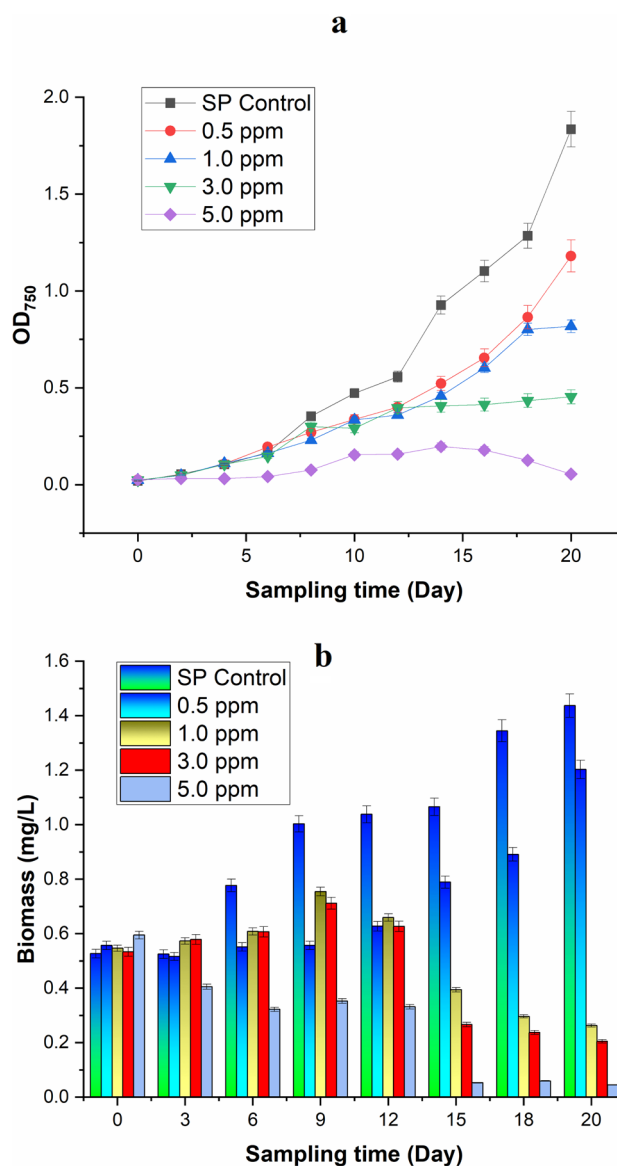


**Fig. 1** a Effect of Cr(VI) on the growth curve of *Spirulina platensis*. All the values were significant at  $P < 0.05$  on ANOVA analysis. b Effect of various Cr(VI) concentrations on biomass yields of *Spirulina platensis*. All the values were significant at  $P < 0.05$  on ANOVA analysis

of these photosynthetic cyanobacteria were notably affected by Cr(VI) concentrations above 0.5 ppm [10] (Fig. 1b).

### Biosorption of Cr(VI) Uptake in *Spirulina platensis*

A higher value of Cr(VI) shows a lesser amount of biosorption than the lower amount of Cr(VI). 5.0-ppm Cr(VI) has 37.723% removal, whereas 42.7%, 45.26%, and 56.56% adsorption were observed in 3.0-ppm, 1.0-ppm, and 0.5-ppm Cr(VI), respectively ( $P < 0.05$ ) (Fig. 2).

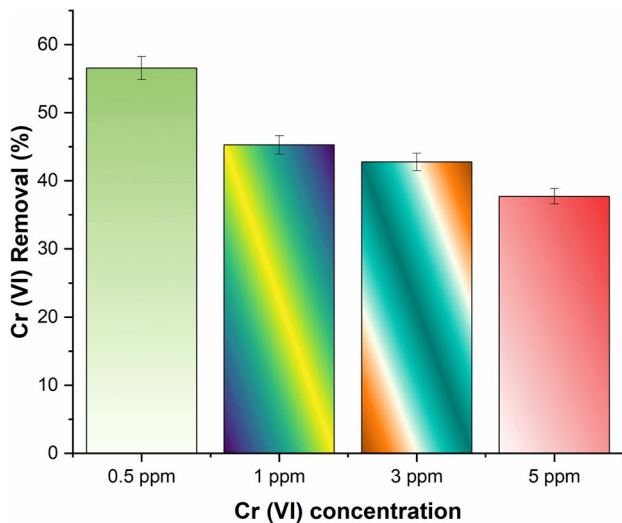


**Fig. 2** Biosorption (percentage removal) of the Cr(VI) in *Spirulina platensis*. All the values were significant at  $P < 0.05$  on ANOVA analysis

### Impact of Cr(VI) on Chlorophyll-a, Carotenoid, and Phycocyanin

Cr(VI) presence significantly affected chlorophyll-a and carotenoid levels, with measured concentrations decreasing with increasing Cr(VI) levels. The amount of chlorophyll-a content (Fig. 3a) was  $4.47 \mu\text{g}/\text{mL}^{-1}$ ,  $3.61 \mu\text{g}/\text{mL}^{-1}$ ,  $2.89 \mu\text{g}/\text{mL}^{-1}$ ,  $1.97 \mu\text{g}/\text{mL}^{-1}$ , and  $1.36 \mu\text{g}/\text{mL}^{-1}$  in control, 0.5 ppm, 1.0 ppm, 3.0 ppm, and 5.0 ppm, respectively (Fig. 3b), whereas the carotenoid content was  $3.94 \mu\text{g}/\text{mL}^{-1}$ ,  $2.16 \mu\text{g}/\text{mL}^{-1}$ ,  $1.36 \mu\text{g}/\text{mL}^{-1}$ ,  $1.09 \mu\text{g}/\text{mL}^{-1}$ , and  $0.55 \mu\text{g}/\text{mL}^{-1}$  in control, 0.5 ppm, 1.0 ppm, 3.0 ppm, and 5.0 ppm, respectively (Fig. 3c) ( $P < 0.05$ ). Phycocyanin content also decreased across the tested Cr(VI) concentrations, indicating substantial physiological impact. The phycocyanin content was recorded at  $3.87 \mu\text{g}/\text{mL}^{-1}$ ,  $2.22 \mu\text{g}/\text{mL}^{-1}$ ,  $1.89 \mu\text{g}/\text{mL}^{-1}$ ,  $1.45 \mu\text{g}/\text{mL}^{-1}$ , and  $1.01 \mu\text{g}/\text{mL}^{-1}$  in control, 0.5 ppm, 1.0 ppm, 3.0 ppm, and 5.0 ppm, respectively ( $P < 0.05$ ).

### Impact of Cr(VI) on Carbohydrate, Protein, and Lipids

Total carbohydrate and protein levels significantly dropped in the presence of Cr(VI), highlighting its detrimental effect on *S. platensis* essential for cell division. The amount of total carbohydrate was  $55.4 \text{ ng}/\text{mL}^{-1}$ ,  $40.35 \text{ ng}/\text{mL}^{-1}$ ,  $28.79 \text{ ng}/\text{mL}^{-1}$ ,  $12.45 \text{ ng}/\text{mL}^{-1}$ , and  $10.5 \text{ ng}/\text{mL}^{-1}$  in control, 0.5 ppm, 1.0 ppm, 3.0 ppm, and 5.0 ppm, respectively ( $P < 0.05$ ) (Fig. 4a) and the protein yield was  $0.45 \text{ ng}/\text{mL}^{-1}$ ,  $0.19 \text{ ng}/\text{mL}^{-1}$ , and  $0.18 \text{ ng}/\text{mL}^{-1}$  in control, 0.5 ppm, and 1.0 ppm, respectively ( $P < 0.05$ ) (Fig. 4b). The reduction in the carbohydrate and protein level in the presence of Cr(VI)

indicates a negative impact on the *S. platensis*, as they are the basic requirements for cell division. Conversely, lipid yield percentage varied across different Cr(VI) concentrations, reflecting adaptive responses to stress. The percentage lipid yield content was  $1.534e + 8 \text{ ng}/\text{mL}^{-1}$ ,  $2.525e + 8 \text{ ng}/\text{mL}^{-1}$ ,  $2.15e + 8 \text{ ng}/\text{mL}^{-1}$ ,  $1.975e + 8 \text{ ng}/\text{mL}^{-1}$ , and  $1.725e + 8 \text{ ng}/\text{mL}^{-1}$  in control, 0.5 ppm, 1.0 ppm, 3.0 ppm, and 5.0 ppm, respectively ( $P < 0.05$ ) (Fig. 4c).

### Fast-Fluorescence Induction

The photo-illumination of the cyanobacteria cells in the responsible actinic light (Using PAM-fluorometer) was used to analyze the kinetics of fluorescence linked to electron transport between PSI and PS II in *S. platensis* at the mid- and late-log phase. The pulse of high irradiance off and on saturated light allows the fluorescence yield. Initial photoluminescence saturation was minimally affected by Cr(VI) toxicity, suggesting negligible impact on the initial fluorescence values and electron transport kinetics between PSI and PSII during mid- and late-log phases, shown in Supplementary Fig. 2. This finding suggests that the primary photochemical processes in the photosynthetic apparatus, particularly those related to the PSII reaction centers, may remain relatively unaffected by low concentrations of chromium. The initial photoluminescence saturation reflects the efficiency of the PSII reaction centers in capturing and utilizing light energy for photosynthesis. When this parameter remains minimally affected by Cr(VI) toxicity, it suggests that certain aspects of the photosynthetic machinery may exhibit resilience to environmental stressors. This resilience of the initial photoluminescence saturation to Cr(VI) toxicity is noteworthy, as it implies that certain aspects of the photosynthetic machinery may maintain functionality even in the presence of environmental stressors.

### Fluorescence Response of the Chlorophyll-a, Carotenoid, and Purified Phycobiliprotein

The fluorescence response varied among the pigments, with chlorophyll-a and carotenoid showing lower fluorescence values compared to phycobiliprotein, indicating differences in photo-acclimation capacity. The estimated maximum chlorophyll fluorescence value ( $F_{m_{chl}}$ ) was 0.42 which is very low as compared to the other pigments (Supplementary Fig. 3a), hence the  $1 \mu\text{g mL}^{-1}$  concentration of cyanobacterial chlorophyll solution showed very slight photo-acclimation. The estimated maximum fluorescence value of carotenoid ( $F_{m_{chl}}$ ) was 0.062 which is very negligible as compared to the other pigments (Supplementary Fig. 3b), hence the  $1 \mu\text{g mL}^{-1}$  concentration of cyanobacterial carotenoid solution showed no photo-acclimation. The

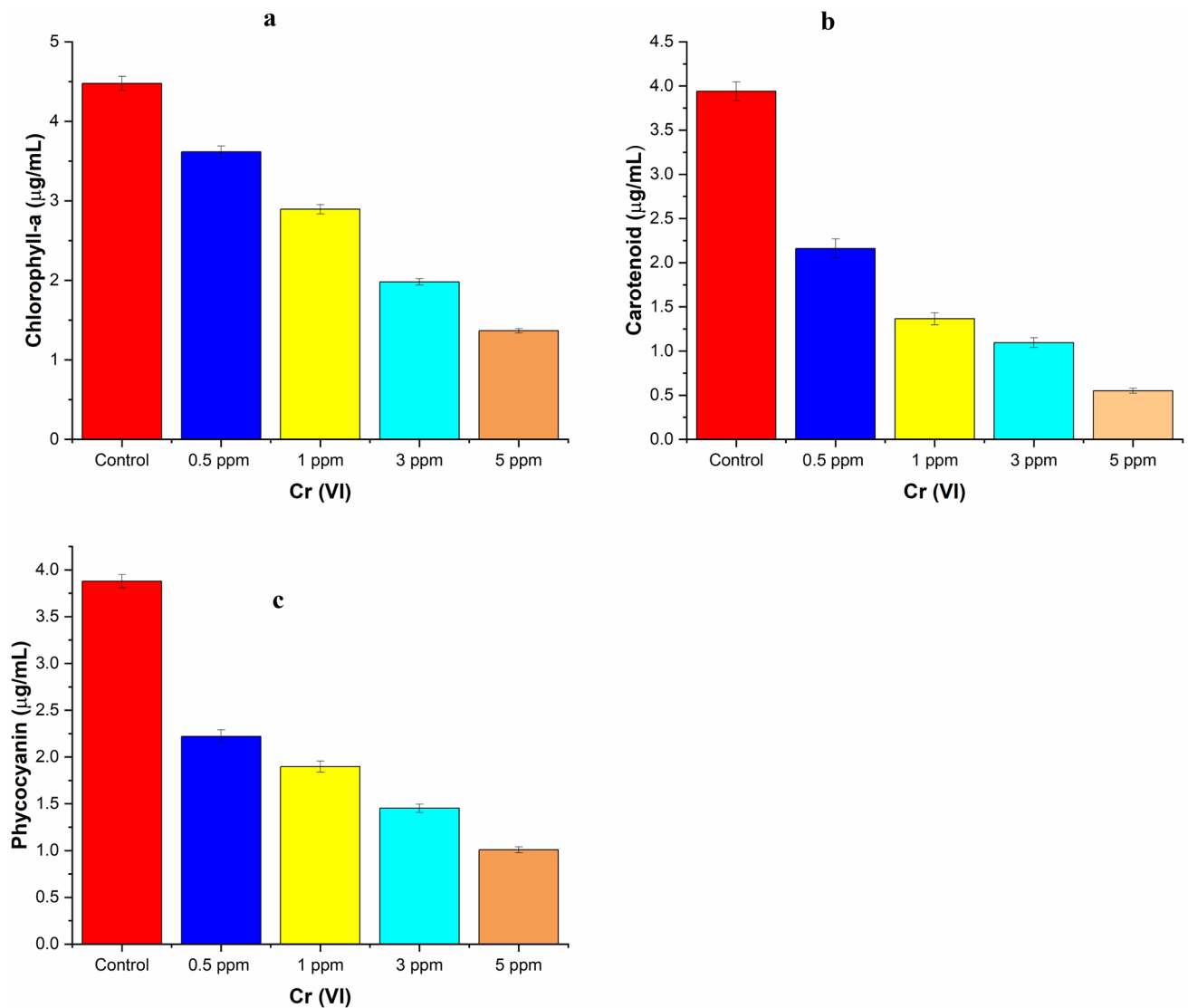


**Fig. 3** Estimation of pigments at various concentrations of the Cr(VI) **a** Chlorophyll-a, **b** Carotenoid, and **c** Phycocyanin. All the values were significant at  $P < 0.05$  on ANOVA analysis

estimated maximum fluorescence value of phycobiliprotein was ( $F_{MPb}$ ) 1.45 (Supplementary Fig. 3c).

### Kautsky Effect and Quenching Analysis

Fluorescence analysis revealed alterations in electron tunneling efficiency at varying Cr(VI) concentrations, affecting photochemical quenching and possibly indicating damage to photosynthetic components at higher Cr(VI) levels. The maximum fluorescence value was highest in untreated *S. platensis*, i.e.,  $F_{M(\text{untreated})}$  0.44. The observed reduction in electronic tunneling force in 0.5 ppm, 1.0 ppm, 3.0 ppm, and 5 ppm was 20.5%, 29.5%, 27.3%, and 36.4%, respectively, which may be because of the alteration of

quantum tunneling of an electron in the downstream process. The highest value of fluorescence was recorded in *S. platensis* at the late exponential phase at saturating and actinic beam. Photochemical quenching value increases in 0.5 ppm & 1 ppm with respect to control. Cr(VI) may be acting here as an alternate electron acceptor intermediate which may be the reason behind the increase in the photochemical quenching. In higher concentrations (3 ppm & 5 ppm), photochemical quenching is highly reduced which may be because of damage to certain essential photosynthesis components. NPQ decrease in the 0.5 ppm & 3.0 ppm is very slight; this means the trace Cr(VI) level (0.5 ppm & 3 ppm) does slightly impact the NPQ analysis [Supplementary Fig. 6a, b (Table 2)].

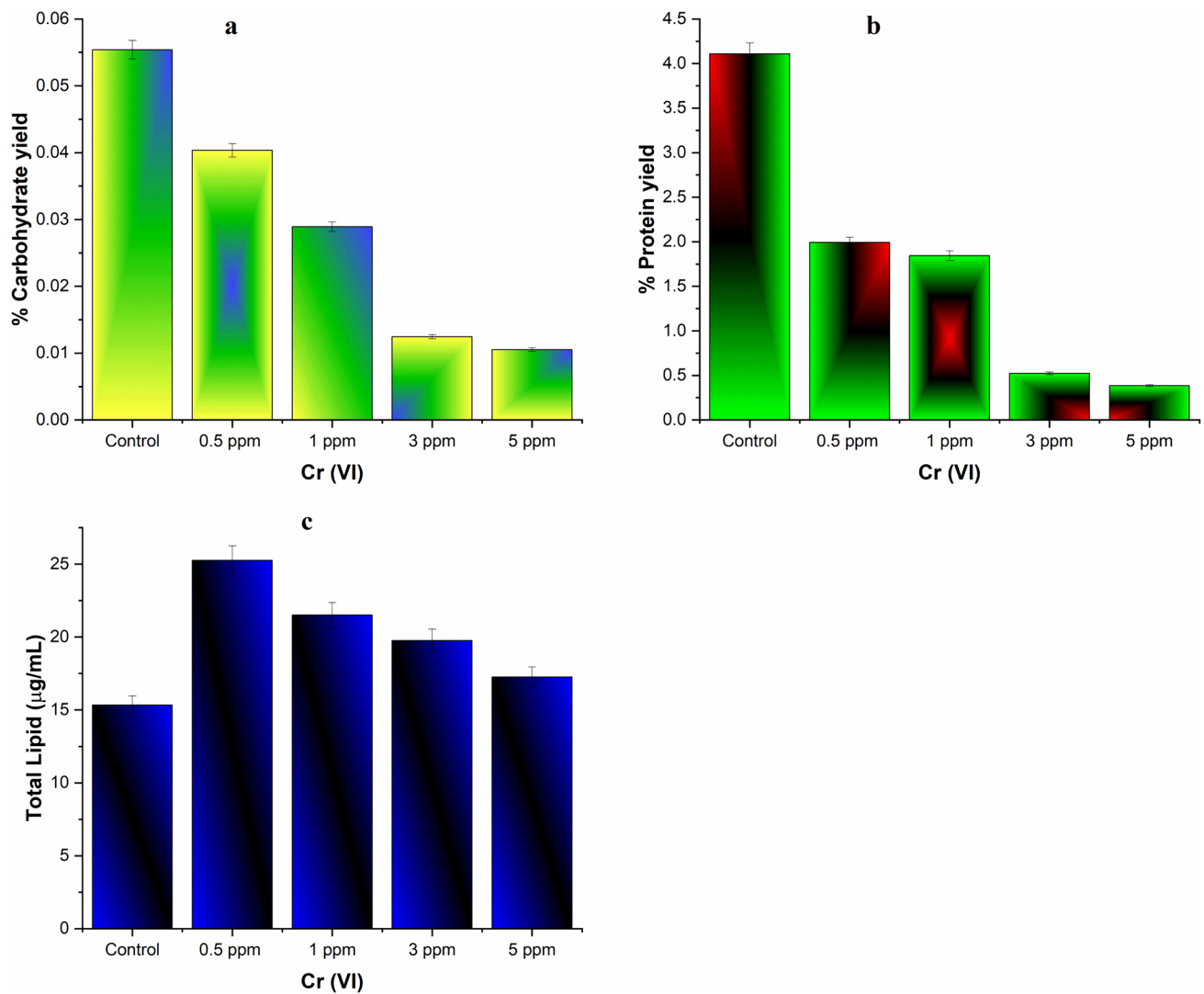


**Fig. 4** Biochemical estimation on the various concentrations of the Cr(VI) in *Spirulina platensis* (values in percentage with SD). **a** Carbohydrate yield, **b** protein yield, and **c** total lipid content. All the values were significant at  $P < 0.05$  on ANOVA analysis

### Photosynthetic Efficiency Analyzer (PEA) and $Q_A$ -Reoxidation

Photosynthetic efficiency is highly reduced while increasing the Cr(VI) level. In 0.5 ppm, 1 ppm, & 3 ppm, the PEA was reduced by 44.78, 42.76, & 38.04%, respectively, while in 5 ppm it is highly reduced by 52.78%. The abrupt change in 5 ppm is visible also in the transient S-state level where it mirrors each other (Table 1). From here it can be assumed that the major reason behind the reduced photosynthesis efficiency may be the interrupted transfer of photons to the adjacent antenna (Supplementary Fig. 4). The  $Q_A$ -Reoxidation indicates the electron flow from PSII to  $Q_A$  reoxidation and vice-versa (Supplementary Fig. 5). These parameters have shown that the reoxidation potential of the microbe in presence of Cr(VI) is gradually reduced as the Cr(VI)

concentration increased (Table 1). The values were recorded at 0.65, 0.64, 0.52, 0.56, and 0.53 for control, 0.5 ppm, 1 ppm, 3 ppm, and 5 ppm, respectively.

### Transient S-States and Meter Analysis

Chromium stress influenced state transitions and photon transfer efficiencies, with significant impacts noted at 5-ppm Cr(VI). A negative peak means that EET from the bulk Chls transfers to the PBSs and the lower Chls. The findings support the Lake Model of photon transfer in *S. platensis*, with Cr(VI) stress leading to observable changes in electron and photon transfer dynamics. The impact of concentration of chromium up to 3 ppm is similar where the transfer of an electron to lower chls is slightly hampered by 11.5% whereas a marginal 27.9% reduction is observed in 5-ppm Cr(VI)

**Table 1** Evaluated value of the maximal fluorescence ( $F_m$ ) in SP at mid-, late-log phase, and exogenous different concentrations of Cr(VI)

Variables	Parameter						
	Fast-fluorescence induction ( $F_M$ )	Kautsky effect ( $F_M$ )	Fluorimeter ( $F_M$ )	$Q_A$ -re-oxidation ( $F_M$ )	PEA ( $F_M$ )	Quenching analysis ( $F_M$ )	Transient S-states ( $F_M$ )
SP at log phase	3.0	0.44	-0.601	-0.65	2.97	0.13	-0.61
0.5 ppm	3.0	0.35	-0.446	-0.64	1.64	0.28	-0.52
1.0 ppm	3.0	0.28	-0.453	-0.52	1.40	0.32	-0.55
3.0 ppm	3.0	0.32	-0.477	-0.56	1.84	0.27	-0.56
5.0 ppm	3.0	0.31	-0.450	-0.53	1.70	0.28	-0.44

concentration. The transfer of photons is shown in Supplementary Fig. 7. The results showed that the state transition is strongly influenced by cellular Cr stress that leads to masks of the state transition. Meter analysis also proves the trend of transient S-states, where the impact of Cr VI at 5.0 ppm was highest, whereas a very slight impact of other concentrations of Cr VI (0.5–3.0 ppm) was observed shown in Supplementary Fig. 8.

### Principal Component Analysis

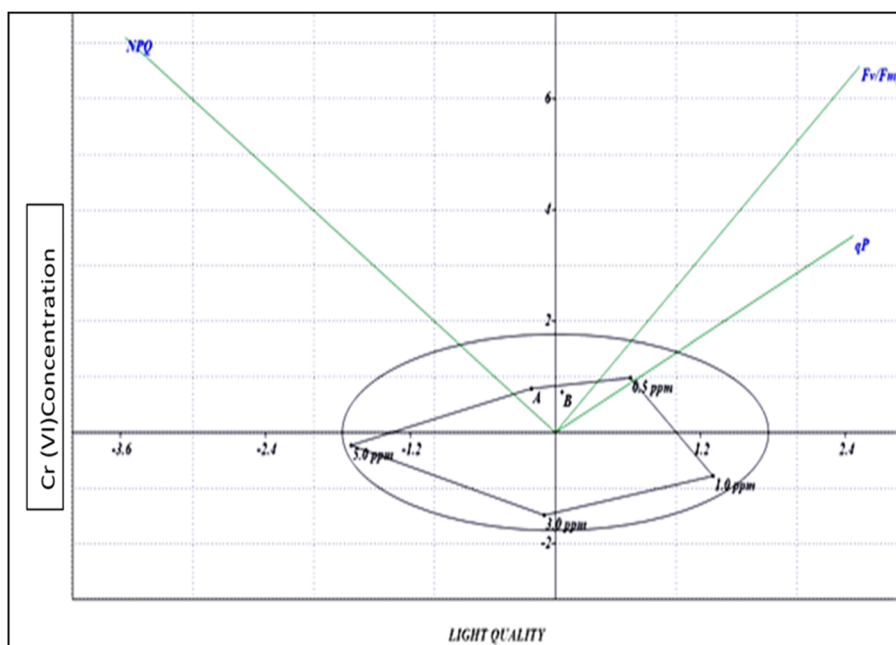
PCA differentiated the effects of Cr(VI) on photosynthetic performance, particularly highlighting the decline in quantum yield and changes in photochemical and non-photochemical quenching with increased Cr(VI) concentrations, assisting in the quick analysis of photosynthetic acclimation and productivity potential in the presence of hexavalent chromium. For all parameters, PCA clearly separated the data into two main components. For photochemical

quenching, non-photochemical quenching, and quantum yield content, respectively, the highest variances of 86.00%, 1.47%, and 85.00% were observed (Fig. 5). The photosynthetic acclimation-producing characteristics were identified by PCA scores decreasing quantum yield performance while adjusting the Cr(VI) concentration of the non-photochemical quenching for the increasing concentration of hexavalent chromium accumulation. PCA was additionally applied in multifactor analysis to quickly analyze the productivity probability area [10].

### Discussion

This research explored the intricate interplay between Cr(VI) stress and the photosynthetic machinery of *Spirulina platensis* and sheds light on the adaptive responses and physiological alterations induced by heavy metal contamination. Photon absorption, electron transfer, and pigment dynamics

**Fig. 5** Principal component analysis at the two independent variable, i.e., light quality and Cr(VI) concentration. All the values were significant at  $P < 0.05$  on ANOVA analysis





intricately regulate the photosynthesis, a fundamental process in sustaining life. The photonic energy is transformed into chemical energy, involving a wide range of microorganisms, including oxygenic cyanobacteria. This process starts when photons are absorbed by antennae and funneled through the PSII reaction centers. The fate of an absorbed photon can be categorized into four pathways: dissipation as heat; transfer to neighboring pigments; photochemical quenching; or fluorescence emission. In photochemical quenching, the photon's energy is utilized in PSII to drive the electron transport chain. The excited electron may return to its ground state, releasing energy as either heat or fluorescence, or it can be transferred to adjacent pigments, such as chlorophyll-a,  $\beta$ -carotenoid, and phycobiliprotein. This energy transition in fluorescence involves the electron moving back to its ground state through vibrational relaxation, passing through several intermediate levels along the way [26–30]. The primary pigments involved in this conversion to photoelectric energy are chlorophyll-a,  $\beta$ -carotenoid, and phycobiliprotein, with each photon absorbed by chlorophyll-a elevating an electron from its ground state [31]. Exposure of cyanobacteria to darkness initiates a slow start in photosynthetic carbon uptake, which is followed by a rapid increase in fluorescence to a quasi-steady state before it decreases again [32–35].

The response of *Spirulina platensis* to varying concentrations of chromium(VI) demonstrates distinct effects, with a notable threshold at 0.5 ppm for chromium(VI) toxicity. Under chromium(VI) stress, distinct patterns emerge, delineating the threshold of toxicity and the consequential physiological shifts within *S. platensis*. Below this concentration, the algae's biomass decreases at a slower rate compared to the control, whereas above 0.5 ppm, there is a significant decline in biomass. The intermediate electron accepting role of 0.5-ppm chromium(VI) potentially explains the observed biomass increase at this concentration by enhancing electron transport and environmental utilization efficiency [10, 13]. However, concentrations exceeding 0.5 ppm appear to inhibit metabolic functions, leading to biomass reduction. The observed threshold effect at 0.5 ppm of chromium(VI) underscores the nuanced response of *S. platensis* to heavy metal exposure. Below this threshold, a moderated increase in biomass is noted, attributed to the potential role of chromium(VI) as an intermediate electron acceptor, enhancing electron transport efficiency. However, concentrations exceeding 0.5 ppm precipitate a marked decline in biomass, indicative of metabolic inhibition and cellular damage. These findings corroborate earlier studies on metal toxicity in *S. platensis*, highlighting the species' sensitivity to environmental contaminants.

Similar observations were made by [36], regarding the impact of lead(II), copper(II), and zinc(II) on *S. platensis*, with notable biomass reduction at 0.2 ppm of these

contaminants. Furthermore, the process of biosorption, vital for Cr(VI) removal, exhibits a concentration-dependent response, with diminished efficacy at higher concentrations. This phenomenon suggests a saturation of binding sites on the surface of *S. platensis* cells, potentially limiting their capacity for Cr(VI) uptake [37]. Such insights into biosorption dynamics have implications for bioremediation strategies, necessitating optimization to enhance metal removal efficiency in contaminated ecosystems [26]. Elevated Cr(VI) levels also impact oxygen evolution, carbon fixation, pigment quality, and cell division, reflected in reduced cell mass and altered growth curves. The study reveals that Cr(VI) affects photosynthesis, with alterations in photo-luminance and photosynthetic activity varying with photon energy frequency.

The impact of chromium(VI) stress on photosynthetic pigments elucidates the intricate balance between light-harvesting and photoprotection mechanisms in *S. platensis*. While chlorophyll-a remains a primary target for photon absorption, secondary pigments such as carotenoids and phycobiliproteins emerge as critical players in mitigating oxidative stress and regulating light acclimation. Table 2 shows that the photo-luminance of Cr(VI) is linked to a drop in photosynthesis activity due to the work function of photon energy, while an increase in photosynthesis activity is seen up to a certain frequency range (per photon energy) in autotrophic organisms [10, 22].

Secondary stress-protecting pigments like carotenoids and phycocyanins, although less abundant than chlorophyll-a, decrease more significantly under Cr(VI) stress. The importance of phycobiliproteins in light harvesting is underscored, especially under higher light conditions, with Cr(VI) exposure altering cell morphology (Fig. 2) and pigment levels. The observed alterations in pigment levels and cell morphology underscore adaptive capacity of cyanobacteria to environmental stressors. The increase in phycobiliproteins is evident in the fluorescence induction parameter, suggesting that the enormous amount of phycobiliprotein in *S. platensis* plays a vital role in photoprotection

**Table 2** Effect of light and dark adapted SP at mid- and late-log samples and exogenous Cr(VI) addition on chlorophyll fluorescence parameters of *Spirulina platensis*

Treatments (PPM)	Chlorophyll fluorescence		
	$F_v/F_m$	$Q_p$	NPQ
SPA	0.73	0.780	1.33
SPB	0.75	0.805	1.29
0.5 ppm	0.85	0.831	1.22
1.0 ppm	0.79	0.866	1.01
3.0 ppm	0.61	0.700	1.16
5.0 ppm	0.531	0.580	1.47

by regulating the light-harvesting mechanism. This is due to the formation of Phycobilisomes, a large peripheral membrane-associated, light-harvesting complex that provides a large surface area for light acclimation [10]. Cr(VI) exposure also leads to reduced carbohydrate and protein levels, essential for cell division, and alters lipid synthesis, indicating a stress response that includes phycobilisome synthesis for photoprotection. The increased amount of total lipids in the presence of Cr(VI) compared to the control shows elevated stress levels leading to the synthesis of phycobilisome in the cell. Lipids are also compounds synthesized to reinforce cell behavior. The reduction in the level of lipid synthesis while increasing the Cr(VI) level from 0.5 to 5.0 ppm indicates a negative impact on lipid metabolism [13, 38].

Moreover, the Kautsky effect and photochemical quenching responses unveil disruptions in electron transfer processes and energy dissipation pathways under Cr(VI) stress. The observed decline in electron flux and photochemical quenching efficiency at higher Cr(VI) concentrations signifies compromised photosynthetic performance and heightened cellular stress. The reduced Kautsky effect suggests that Cr(VI) is affecting the flux transfer from PSII to  $Q_A$  or  $Q_A$  to the reaction center, requiring further investigation. The synthesis of carbohydrates utilizing electronic energy generates the major flux, which functions as the driving force for the electron's movement in the reaction center [39]. The reduced levels of carbon fixation are evident in the decreased levels of biomass in the presence of Cr(VI). Therefore, Cr(VI) is influencing the system's electron flux. The reduced  $Q_A$  reoxidation also supports this claim. The photosynthesis cycle commences after photonic energy is absorbed by PSII. This energy is then utilized to transfer an electron from the S-cycle [36]. Hence, the decrease in the electron flux in the cycle will also affect the S-state, as evidenced by the Transient S-state observations. Importantly, the reduction is not on par with the parameters within the cycle, indicating that Cr(VI) does not affect the S-complex's electron transfer to PSII, at least in *S. platensis*. Thus, Cr(VI) is directly influencing the primary quantum level phenomenon: coherence and tunneling [40]. The coherence of the state means the exciton can detect multiple pathways of the energy landscape simultaneously and determine the most efficient route, resulting in an efficient energy transfer process. Both quantum coherence and quantum tunneling work together to find the best possible route for the electron to reach the final electron acceptor without losing its energy [41]. However, the decreased levels of  $Q_A$  reoxidation, Kautsky fluorescence, and biomass indicate that Cr(VI) is directly influencing the positioning of the micro-array of the photosystem's multiple components, affecting the quantum coherence and quantum tunneling phenomenon. This mechanism is also observed in the photochemical quenching (PQ) response. At low levels of Cr(VI), PQ appears to enhance,

while at higher levels, it is observed to decrease. Cr(VI) may act as an intermediate electron acceptor, which is why photochemical quenching increases. At higher concentrations (3 ppm & 5 ppm), photochemical quenching is significantly reduced, indicating permanent damage to essential photosynthesis components. Excess photonic energy, which cannot be easily accommodated by the photosystem machinery, is dissipated as heat, which can be quantified by the non-photochemical quenching (NPQ) [42]. PQ is highly increased at 5 ppm, indicating that 5-ppm Cr(VI) significantly increases heat loss in the microorganism, reducing photosynthesis efficiency. Therefore, it can be assumed that higher concentrations of Cr(VI) introduce a high-stress level in the organism, causing them to route light energy into heat dissipation [43–46]. These findings also highlight the complex interaction between quantum coherence, electron tunneling, and photoprotective mechanisms in *S. platensis*, offering valuable insights into the molecular underpinnings of metal-induced phototoxicity.

However, it is essential to acknowledge potential limitations in the experimental design, such as the reliance on laboratory-based assays and simplified growth conditions. Additionally, extrapolating findings from *S. platensis* to broader ecological contexts warrants caution, considering the species-specific responses to Cr(VI) stress. The findings emphasize the need for further research to explore the detailed molecular mechanisms underlying these responses, with implications for improving the resilience of *S. platensis* and other microalgae to environmental contaminants. Future research endeavors should aim to elucidate the molecular mechanisms underlying metal-induced toxicity and explore potential synergies with microbial consortia for enhanced bioremediation efficacy [47–50].

## Conclusion

Our study on *S. platensis* responses to Cr(VI) stress offers valuable insights into the intricate mechanisms of metal tolerance, spanning physiological, biochemical, and molecular adaptations. These findings advance our understanding of algal biology under heavy metal stress and underscore the potential of Spirulina-based bioremediation strategies in contaminated environments. The investigation into transient S-states revealed a distinct mechanism by which higher concentrations of Cr(VI) disrupt the quantum leap process, impairing the organism's viability. Interestingly, lower Cr(VI) concentrations (0.5 and 1.0 ppm) appeared to enhance photochemical quenching, suggesting a nuanced role of Cr(VI) as an intermediate electron acceptor. Microscopic analysis corroborated these findings, highlighting morphological changes induced by elevated Cr(VI) levels.

Moreover, the observed high non-photochemical quenching values underscored the rapid dissipation of absorbed electronic energy as heat, indicative of hindered exciton energy transfer in the presence of high Cr(VI) concentrations. Data from the Photosynthetic Efficiency Analyzer (PEA) provided quantitative insights into how these alterations in morphology and electrical characteristics directly impact the photosynthetic efficiency of *S. platensis*. While our study contributes significantly to our understanding of metal–algal interactions, it is essential to acknowledge its limitations. The reliance on laboratory-based assays and simplified growth conditions may not fully capture the complexities of real-world ecosystems. Future research endeavors should aim to elucidate the molecular mechanisms underlying metal-induced toxicity and explore potential synergies with microbial consortia for enhanced bioremediation efficacy. Future research should also focus on refining bioremediation strategies utilizing *S. platensis* and other microorganisms in contaminated environments. Additionally, efforts to characterize the molecular basis of metal tolerance mechanisms in algae hold promise for the development of targeted interventions to mitigate metal pollution challenges and safeguard aquatic ecosystems.

**Supplementary Information** The online version contains supplementary material available at <https://doi.org/10.1007/s00284-024-03743-4>.

**Acknowledgements** The management/executive authority of Nehru Gramme Bharati (Deemed to be University), Prayagraj has our deepest gratitude for giving seed funding for the experiment, for which the authors are grateful.

**Author Contributions** Shanthy Sundaram and Adi Nath provided the experimental designs. Adi Nath was carrying out the experiments. Abhijeet Sharma and Shailendra Kumar Singh offered manuscript drafting assistance to Adi Nath, who also prepared the initial draft. Shanthy Sundaram contributed to the manuscript by reviewing and providing feedback for improvement.

**Funding** Not applicable.

**Data Availability** It will be provided on request.

## Declarations

**Competing Interests** The authors declare that they have no known competing financial interests or personal relationships that could have appeared to influence the work reported in this paper.

**Ethical Approval** Not applicable.

**Consent of Participate** Not applicable.

**Code Availability** Not applicable.

**Consent for Publication** Not applicable.

## References

- Singh SK, Bansal A, Jha MK, Dey A (2012) An integrated approach to remove Cr(VI) using immobilized *Chlorella minutissima* grown in nutrient rich sewage wastewater. *Bioresour Technol* 104:257–265. <https://doi.org/10.1016/j.biortech.2011.11.044>
- Sharma A, Maurya N, Singh SK, Sundaram S (2024) Investigation on synergetic strategy for the rejuvenation of Cr(VI) contaminated soil using biochar-immobilized bacteria and cyanobacteria consortia. *J Environ Chem Eng* 12(2):112034. <https://doi.org/10.1016/j.jece.2024.112034>
- Tumolo M, Ancona V, De Paola D, Losacco D, Campanale C, Massarelli C, Uricchio VF (2020) Chromium pollution in European water, sources, health risk, and remediation strategies: an overview. *Int J Environ Res Public Health* 17(15):5438. <https://doi.org/10.3390/ijerph17155438>
- Stirbet A (2011) On the relation between the Kautsky effect (chlorophyll a fluorescence induction) and photosystem II: basics and applications of the OJIP fluorescence transient. *J Photochem Photobiol B* 104(1–2):236–257. <https://doi.org/10.1016/j.jphotobiol.2010.12.010>
- Prasanna R, Jaiswal P, Kaushik BD (2008) A cyanobacterium as potential options for environmental sustainability—promises and challenges. *Indian J Microbiol* 48(1):89–94. <https://doi.org/10.1007/s12088-008-0009-2>
- Bashir KMI, Lee HJ, Mansoor S, Jahn A, Cho MG (2021) The effect of chromium on photosynthesis and lipid accumulation in two chlorophyte microalgae. *Energies* 14(8):2260. <https://doi.org/10.3390/en14082260>
- Sena L, Rojas D, Montiel E, González H, Moret J, Naranjo L (2011) A strategy to obtain axenic cultures of *Arthrospira* spp. cyanobacteria. *World J Microbiol Biotechnol* 27:1045–1053. <https://doi.org/10.1007/s11274-010-0549-6>
- Perreault F, Ali NA, Saison C, Popovic R, Juneau P (2009) Dichromate effect on energy dissipation of photosystem II and photosystem I in *Chlamydomonas reinhardtii*. *J Photochem Photobiol B* 96(1):24–29. <https://doi.org/10.1016/j.jphotobiol.2009.03.011>
- Nath A, Rahman A, Singh SK, Dixit K, Sundaram S (2015) Chromium induced alterations in different individual microalga and their consortia. *Indian J Nat Sci* 6:10177–10189
- Nath A, Tiwari PK, Rai AK, Sundaram S (2017) Microalgal consortia differentially modulate progressive adsorption of hexavalent chromium. *Physiol Mol Biol Plants* 23:269–280. <https://doi.org/10.1007/s12298-017-0415-1>
- Kumar KS, Dahms HU, Lee JS, Kim HC, Lee WC, Shin KH (2014) Algal photosynthetic responses to toxic metals and herbicides assessed by chlorophyll a fluorescence. *Ecotoxicol Environ Saf* 104:51–71. <https://doi.org/10.1016/j.ecoenv.2014.01.042>
- Nath A, Tiwari PK, Rai AK, Sundaram S (2019) Evaluation of carbon capture in competent microalgal consortium for enhanced biomass, lipid, and carbohydrate production. *3 Biotech* 9(11):379. <https://doi.org/10.1007/s13205-019-1910-6>
- Sharma A, Singh SK, Sundaram S (2024) Efficient biosequestration of Cr(VI) by *Bacillus* spp. SSAU-2: optimization, mathematical modelling, and plant growth promotion. *Biochem Eng J* 204:109186. <https://doi.org/10.1016/j.bej.2023.109186>
- Mackinney G (1941) Absorption of light by chlorophyll solutions. *J Biol Chem* 140(2):315–322. [https://doi.org/10.1016/S0021-9258\(18\)51320-X](https://doi.org/10.1016/S0021-9258(18)51320-X)
- Siegelman HW, Kycia JH (1982) Molecular morphology of cyanobacterial phycobilisomes. *Plant Physiol* 70(3):887–897. <https://doi.org/10.1104/pp.70.3.887>
- Zavafer A, González-Solís A, Palacios-Bahena S, Saucedo-García M, Tapia de Aquino C, Vázquez-Santana S et al (2020) Organized

- disassembly of photosynthesis during programmed cell death mediated by long chain bases. *Sci Rep* 10(1):10360. <https://doi.org/10.1038/s41598-020-65186-8>
17. Urrejola C, von Dassow P, van den Engh G, Salas L, Mullineaux CW, Vicuña R, Sánchez-Baracaldo P (2020) Loss of filamentous multicellularity in cyanobacteria: the extremophile *Gloeocapsopsis* sp. strain UTEX B3054 retained multicellular features at the genomic and behavioral levels. *J Bacteriol* 202(12):e00514-19. <https://doi.org/10.1128/jb.00514-19>
  18. Strieth D, Di Nonno S, Stiefelmaier J, Kollmen J, Geib D, Ulber R (2021) Co-cultivation of diazotrophic terrestrial cyanobacteria and *Arabidopsis thaliana*. *Eng Life Sci* 21(3–4):126–136. <https://doi.org/10.1002/elsc.202000068>
  19. Baker NR (2008) Chlorophyll fluorescence: a probe of photosynthesis *in vivo*. *Annu Rev Plant Biol* 59:89–113. <https://doi.org/10.1146/annurev.arplant.59.032607.092759>
  20. Sharma A, Singh SK, Nath A, Sundaram S (2024) Methyl red biodegradation by novel halophilic *Lactiplantibacillus plantarum* SS-AU1 isolated from river Ganges. *Int J Environ Sci Technol*. <https://doi.org/10.1007/s13762-024-05468-0>
  21. Maxwell K, Johnson GN (2000) Chlorophyll fluorescence—a practical guide. *J Exp Bot* 51:659–668. <https://doi.org/10.1093/jexbot/51.345.659>
  22. Tiwari PK, Singh AK, Singh VP, Prasad SM, Ramawat N, Tripathi DK et al (2019) Liquid assisted pulsed laser ablation synthesized copper oxide nanoparticles (CuO-NPs) and their differential impact on rice seedlings. *Ecotoxicol Environ Saf* 176:321–329. <https://doi.org/10.1016/j.ecoenv.2019.01.120>
  23. Yemm EW, Willis A (1954) The estimation of carbohydrates in plant extracts by anthrone. *Biochem J* 57(3):508. <https://doi.org/10.1042/bj0570508>
  24. Lowry O, Rosebrough N, Farr AL, Randall R (1951) Protein measurement with the Folin phenol reagent. *J Biol Chem* 193(1):265–275
  25. Bligh EG, Dyer WJ (1959) A rapid method of total lipid extraction and purification. *Can J Biochem Physiol* 37(8):911–917. <https://doi.org/10.1139/o59-099>
  26. Bailey S, Grossman A (2008) Photoprotection in cyanobacteria: regulation of light-harvesting. *Photochem Photobiol* 84(6):1410–1420. <https://doi.org/10.1111/j.1751-1097.2008.00453.x>
  27. Gilmore AM, Hazlett TL, Debrunner PG, Govindjee (1996) Comparative time-resolved photosystem II chlorophyll fluorescence analyses reveal distinctive differences between photoinhibition reaction centre damage and xanthophyll cycle-dependent energy dissipation. *Photochem Photobiol* 64(3):552–563. <https://doi.org/10.1111/j.1751-1097.1996.tb03105.x>
  28. Pfündel EE (2021) Simultaneously measuring pulse-amplitude-modulated (PAM) chlorophyll fluorescence of leaves at wavelengths shorter and longer than 700 nm. *Photosynth Res* 147(3):345–358. <https://doi.org/10.1007/s11120-021-00821-7>
  29. Lakatos GE, Ranglová K, Manoel JC, Grivalský T, Masojídek J (2021) Photosynthetic monitoring techniques indicate maximum glycogen accumulation in nitrogen-limited *Synechocystis* sp. PCC 6803 culture. *Algal Res* 55:102271. <https://doi.org/10.1016/j.algal.2021.102271>
  30. Hassannejad S, Lotfi R, Ghafarbi SP, Oukarroum A, Abbasi A, Kalaji HM, Rastogi A (2020) Early identification of herbicide modes of action by the use of chlorophyll fluorescence measurements. *Plants* 9(4):529. <https://doi.org/10.3390/plants9040529>
  31. Dąbrowski P, Baczewska-Dąbrowska AH, Bussotti F, Pollastri M, Piekut K, Kowalik W et al (2021) Photosynthetic efficiency of *Microcystis* ssp. under salt stress. *Environ Exp Bot* 186:104459. <https://doi.org/10.1016/j.envexpbot.2021.104459>
  32. Küpper H, Benedikty Z, Morina F, Andresen E, Mishra A, Trtílek M (2019) Analysis of OJIP chlorophyll fluorescence kinetics and  $Q_A$  reoxidation kinetics by direct fast imaging. *Plant Physiol* 179(2):369–381. <https://doi.org/10.1104/pp.18.00953>
  33. Chen Z, Song S, Wen Y (2016) Reduction of Cr(VI) into Cr(III) by organelles of *Chlorella vulgaris* in aqueous solution: an organelle-level attempt. *Sci Total Environ* 572:361–368. <https://doi.org/10.1016/j.scitotenv.2016.07.217>
  34. Torres MA, Ritchie RJ, Lilley RMCC, Grillet C, Larkum AWD (2014) Measurement of photosynthesis and photosynthetic efficiency in two diatoms. *N Z J Bot* 52(1):6–27. <https://doi.org/10.1080/0028825X.2013.831917>
  35. Choudhary M, Jetley UK, Khan MA, Zutshi S, Fatma T (2007) Effect of heavy metal stress on proline, malondialdehyde, and superoxide dismutase activity in the cyanobacterium *Spirulina platensis*-S5. *Ecotoxicol Environ Saf* 66(2):204–209. <https://doi.org/10.1016/j.ecoenv.2006.02.002>
  36. Colla LM, Dal’Magro C, De Rossi A, Thomé A, Reinehr CO, Bertolin TE, Costa JAV (2015) Potential of live *Spirulina platensis* on biosorption of hexavalent chromium and its conversion to trivalent chromium. *Int J Phytoremed* 17(9):861–868. <https://doi.org/10.1080/15226514.2014.964846>
  37. Simon PS, Makita H, Bogacz I, Fuller F, Bhowmick A, Hussein R et al (2023) Capturing the sequence of events during the water oxidation reaction in photosynthesis using XFELs. *FEBS Lett* 597(1):30–37. <https://doi.org/10.1002/1873-3468.14527>
  38. Faisal M, Hameed A, Hasnain S (2005) Chromium-resistant bacteria and cyanobacteria: impact on Cr(VI) reduction potential and plant growth. *J Ind Microbiol Biotechnol* 32(11–12):615–621. <https://doi.org/10.1007/s10295-005-0241-2>
  39. Holt NE, Fleming GR, Niyogi KK (2004) Toward an understanding of the mechanism of nonphotochemical quenching in green plants. *Biochemistry* 43:8281–8289. <https://doi.org/10.1021/bi0494020>
  40. Rawsthorne S (2002) Carbon flux and fatty acid synthesis in plants. *Prog Lipid Res* 41(2):182–196. [https://doi.org/10.1016/S0163-7827\(01\)00023-6](https://doi.org/10.1016/S0163-7827(01)00023-6)
  41. Mančal T (2020) A decade with quantum coherence: how our past became classical and the future turned quantum. *Chem Phys* 532:110663. <https://doi.org/10.1016/j.chemphys.2019.110663>
  42. Tao MJ, Zhang NN, Wen PY, Deng FG, Ai Q, Long GL (2020) Coherent and incoherent theories for photosynthetic energy transfer. *Sci Bull* 65(4):318–328. <https://doi.org/10.1016/j.scib.2019.12.009>
  43. Murchie EH, Ruban AV (2020) Dynamic non-photochemical quenching in plants: from molecular mechanism to productivity. *Plant J* 101(4):885–896. <https://doi.org/10.1111/tbj.14601>
  44. Kaamouh M, El-Agawany N, Salhin HE, El-Zeiny A (2022) Monitoring effect of nickel, copper, and zinc on growth and photosynthetic pigments of *Spirulina platensis* with suitability investigation in Idku Lake. *Environ Sci Pollut Res* 29(52):78942–78959. <https://doi.org/10.1007/s11356-022-21328-1>
  45. Schreiber U, Klughammer C (2021) Evidence for variable chlorophyll fluorescence of photosystem I *in vivo*. *Photosynth Res*. <https://doi.org/10.1007/s11120-020-00814-y>
  46. Santos-Merino M, Torrado A, Davis GA, Röttig A, Bibby TS, Kramer DM, Ducat DC (2021) Improved photosynthetic capacity and photosystem I oxidation via heterologous metabolism engineering in cyanobacteria. *Proc Natl Acad Sci USA*. <https://doi.org/10.1073/pnas.2021523118>
  47. Horton P, Johnson MP, Perez-Bueno ML, Kiss AZ, Ruban AV (2008) Photosynthetic acclimation: does the dynamic structure and macro-organization of photosystem II in higher plant grana membranes regulate light harvesting states? *FEBS J*

- 275(6):1069–1079. <https://doi.org/10.1111/j.1742-4658.2008.06263.x>
48. Radakovits R, Jinkerson RE, Darzins A, Posewitz MC (2010) Genetic engineering of algae for enhanced biofuel production. *Eukaryot Cell* 9:486–501. <https://doi.org/10.1128/ec.00364-09>
  49. Munoz R, Guieysse B (2006) Algal-bacterial processes for the treatment of hazardous contaminants: a review. *Water Res* 40:2799–2815. <https://doi.org/10.1016/j.watres.2006.06.011>
  50. Musah BI, Xu Y, Liang C, Peng L (2022) Biosorption of chromium(VI), iron(II), copper(II), and nickel(II) ions onto alkaline modified *Chlorella vulgaris* and *Spirulina platensis* in binary systems. *Environ Sci Pollut Res* 29(41):62514–62536. <https://doi.org/10.1007/s11356-022-19725-7>

**Publisher's Note** Springer Nature remains neutral with regard to jurisdictional claims in published maps and institutional affiliations.

Springer Nature or its licensor (e.g. a society or other partner) holds exclusive rights to this article under a publishing agreement with the author(s) or other rightsholder(s); author self-archiving of the accepted manuscript version of this article is solely governed by the terms of such publishing agreement and applicable law.